ОБЪЕДИНЕННЫЙ
ИНСТИТУТ
ЯДЕРНЫХ
ИССЛЕДОВАНИЙ

Дубна

E7-2000-305

A.G.Artukh, G.F.Gridnev, M.Gruszecki[1], F.Koscielniak[1],
A.G.Semchenkov[2], O.V.Semchenkova[2], Yu.M.Sereda[2],
J.Szmider[1], Yu.G.Teterev

FORWARD ANGLE YIELDS OF ISOTOPES WITH $2 \leq Z \leq 11$ IN THE REACTION OF ^{18}O (35 · A MeV) WITH ^{9}Be

Submitted to «Ядерная физика»

[1]Henryk Niewodniczanski Institute of Nuclear Physics, Cracow, Poland
[2]Permanent address: Institute for Nuclear Research, Kyiv, Ukraine

2000

1 Introduction

The availability of heavy ions in the intermediate energy offers a unique opportunity for detailed studies of transition energy region [1] between low energy nuclear collisions [2] and high energy multifragmentation processes [3]. In the transition region (20 to 100·A MeV) the projectile velocities are comparable to the characteristic velocities in nuclear matter such as the velocity of sound and the Fermi velocity of nucleons inside nuclei. Overcoming these threshold velocities can hope to meet qualitatively new phenomena. There still remains an open question: how rapidly do reaction mechanisms of the binary type (characteristic for the low energy regime) evolve in the multifragmentation desintegration of colliding partners (characteristic for the high energy regime)? The possible influence of the neutron excess $(N/Z)_p$ of the projectile and of the $(N/Z)_t$ of the target on the production cross section of unstable nuclei remains also unknown. It is well known that weakly-bound drip-line isotopes are synthesized with maximum yields in nucleus-nucleus collisions at intermediate energies [4, 5]. What reaction mechanisms are dominant in the processes of producing the "cold" drip-line isotopes at intermediate energies?

Now there are many experimental data related to the investigation of the reaction mechanisms in the region of intermediate energies but the main data have been obtained in large angle measurements [1, 6-11]. As a rule, the fragments emitted outside the zero-angle (large angles) are produced in nucleus-nucleus collisions with large transferred traverse momenta (big losses of kinetic energy) or in multifragmentation processes. Such experiments are not sensitive to the "quasi-elastic" process of producing the weakly-bound (drip-line) isotopes.

To fill the gap in our knowledge, it is necessary to study the evolution of the reaction mechanisms of producing the weekly-bound nuclei as a function of projectile energy in nucleus-nucleus collisions with different entry mass and charge asymmetry. Moreover, the experimental information to be obtained is very important for choosing the optimal energy and projectile-target combination needed to synthesize unknown drip-line nuclei and to form intensive secondary radioactive beams.

The aim of this work is:

- to study the yields of charged reaction products focusing the main attention on the production of near drip-line nuclei using the ^{18}O projectile in the Fermi energy domain (35·A MeV) and the light ^{9}Be target effectively used in the reactions of synthesis of the drip-line nuclei,

- to determine the intensity of secondary radioactive beams of halo-like nuclei of ^{11}Li, ^{12}Be and ^{14}Be.

Taking into account that weakly-bound neutron drip-line isotopes could survived only when they are induced in "soft" peripheral nuclear collisions with a minimum transferred traverse momentum (minimum excitation energy), the kinematic separator COMBAS is used in zero angle spectrometry of charged reaction products [12]. The peculiarities of the beam-direct spectrometry of charged particles are presented in Appendix.

2 Experimental conditions

The 14 mg/cm^2 ^{9}Be target foil was irradiated with the 35·A MeV ^{18}O particle beam of up to 2 μA (electric) intensity produced on the U-400M cyclotron at the Flerov Laboratory of Nuclear Reactions, JINR. The target was placed at the entrance focus of the COMBAS separator (Fig.1). The diameter of the beam spot on the target did not exceed 3 mm.

The nuclear products emitted at forward angles within a COMBAS solid angle(6 mstr) were separated from the intense beam of bombarding particles by magnetic rigidity and identified on the mass number A and atomic number Z by the (ΔE, E) telescope [13, 14] placed at the exit achromatic focus of the COMBAS separator. The measurements of the yields of isotopes were carried out by scanning the range of magnetic rigidities covering the velocity distributions of the studied isotopes of the light elements with $2 \leq Z \leq 11$. The magnetic fields of all the 8 magnets of the separator were measured with Hall probes. The ^{18}O primary beam was transmitted along the ion-optic axis of the separator to determine the beam magnetic rigidity and to use it as momentum reference in the measurements of momentum distributions (or velocity distributions) of charged products. The thickness of the Be target was controlled by the primary beam magnetic rigidity with the installed target and without it. Proportional counters were placed behind the target on the both sides of the beam axis to monitor the beam intensity and beam position on the target. The target was also used to measure the beam current.

In the F_d dispersive focal plane the 2 mm slit on the ion-optics axis of the separator was positioned to limit the momentum acceptance within 0.15% and to decrease the load of the electronics and read-out system near the beam

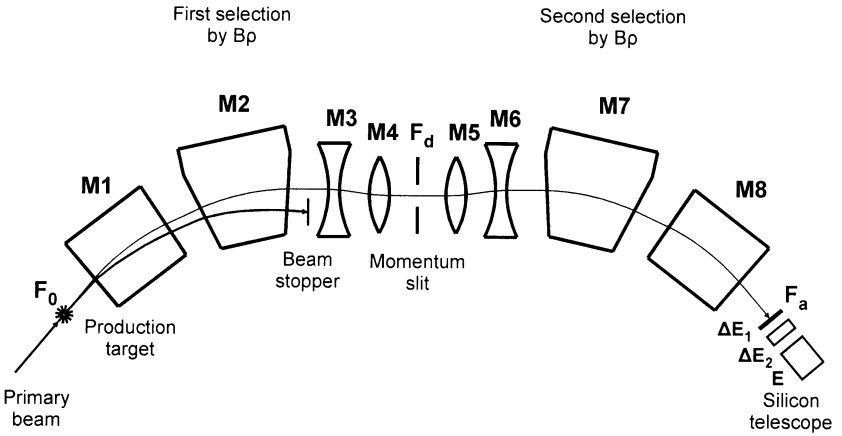

CONFIGURATION	ΔΩ (msr)	Δp/p (%)	Bρ (T·m)	$R_{p/\Delta p}$	L (m)
$M_1M_2M_3M_4F_dM_5M_6M_7M_8F_a$	6.4	±10	4.5	4360	14.5

Fig.1. Schematic drawing of the COMBAS secondary beam facility. At the bottom of the table the main ion-optics parameters of the COMBAS kinematic separator are presented.

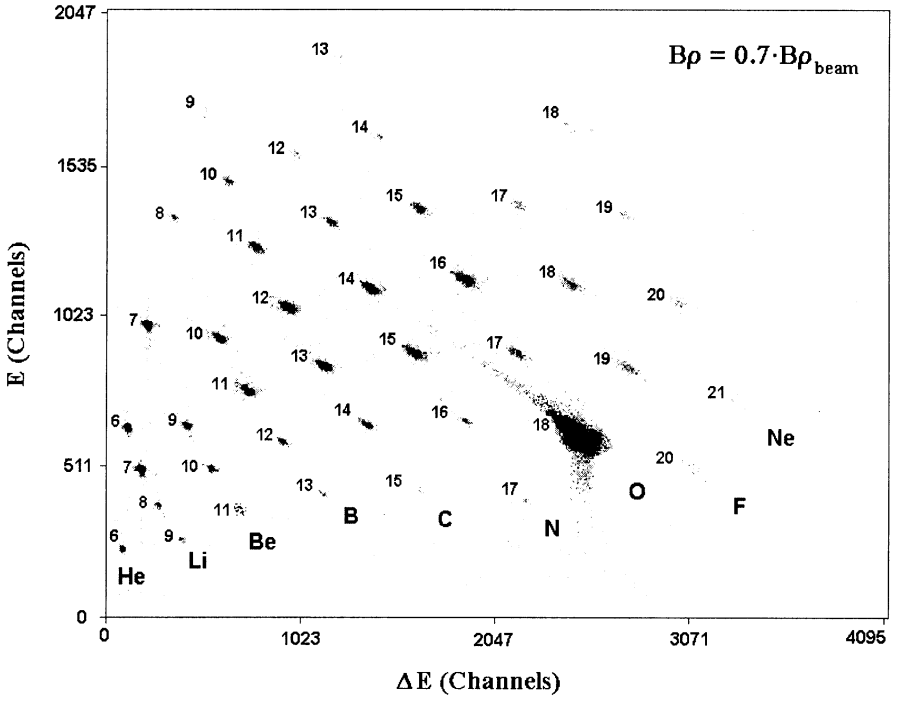

Fig.2. Identification two-dimensional plot of residue energy E versus energy loss ΔE for $B\rho = 0.7 \cdot B\rho_{beam}$ setting (for example) The numbers near each group of events marks the mass numbers of isotopes of the indicated elements (at the bottom).

magnetic rigidity. In the same F_d plane a thin stripping 24 μm mylar foil was installed to remove products whose ionic charge differed from the nuclear charge. The proximity to the beam magnetic rigidity was limited by the ratio $B\rho/B\rho_{beam} = 0.98$ and $B\rho/B\rho_{beam} = 1.01$. The products were detected in the F_a achromatic focus by a telescope consisting of silicon detectors: ΔE1 (0.38 mm, 60 x 60 mm^2), ΔE2 (3.5 mm, $\emptyset$60 mm), E (7.5 mm, $\emptyset$60 mm), and identified by the nuclear charge and mass number using a combination of two methods: magnetic rigidity and (ΔE, E):

$$E = (B\rho)^2 \cdot Z^2/A, \tag{1}$$

$$\Delta E \approx A \cdot Z^2/E \tag{2}$$

where A, Z and E are the mass number, atomic number and energy of the detected product, respectively. The isotopic identification quality of used combination is seen from the Fig.2.

The yields of all the isotopes are represented in relative units after normalization of registered isotopic events to the monitor detector counting.

3 Experimental results

3.1 Forward-angle inclusive velocity distributions of the products

The inclusive forward-angle velocity distributions of the isotopes with the atomic number $2 \leq Z \leq 11$ induced in the reaction of 35·A MeV ^{18}O on the ^{9}Be target are shown in Figs.3-6. The isotopic velocity V is referred to that of

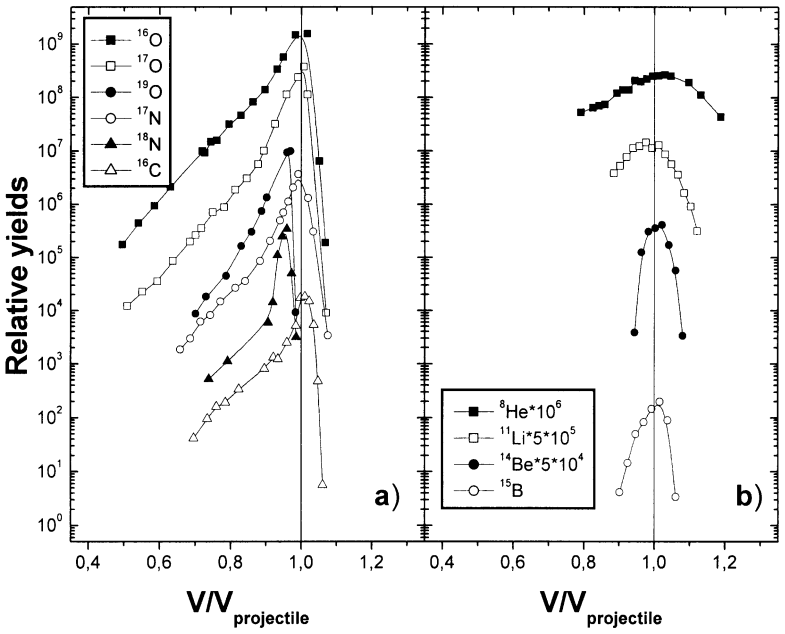

Fig.3. The forward-angle inclusive velocity distributions (relative yields) of the isotopes produced in small nucleonic transfer reactions (Fig.3a). The same for the isotopes produced in stripping proton reactions (Fig.3b). The isotope velocity V is referred to the projectile velocity $V_{projectile}$. The numbers near the isotopic symbols (in the frame) show the multiplied factors of the experimental yields (for visual convenience).

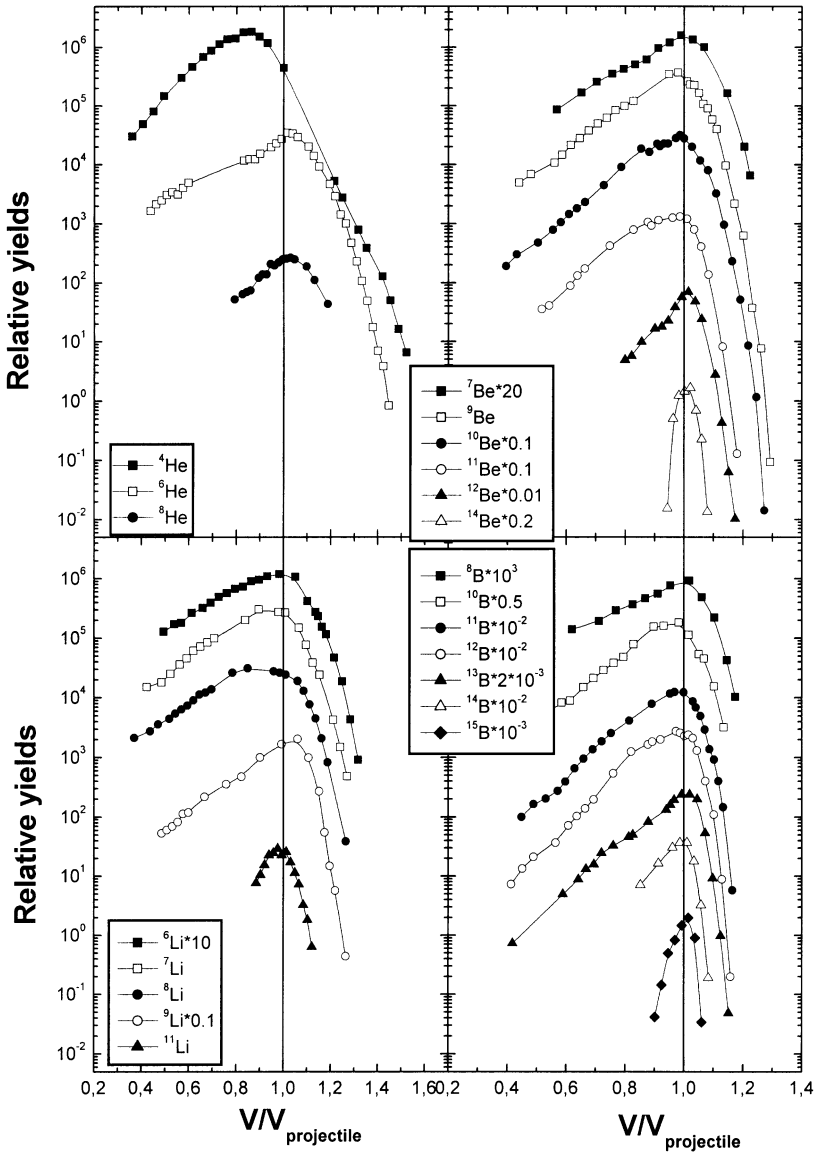

Fig.4. The forward-angle inclusive velocity distributions (relative yields) of the isotopes He, Li, Be and B. The isotope velocity V is referred to that of the beam $V_{projectile}$. The numbers near isotopes (in frame) show the multiplied factors of the experimental yields (for visual convenience).

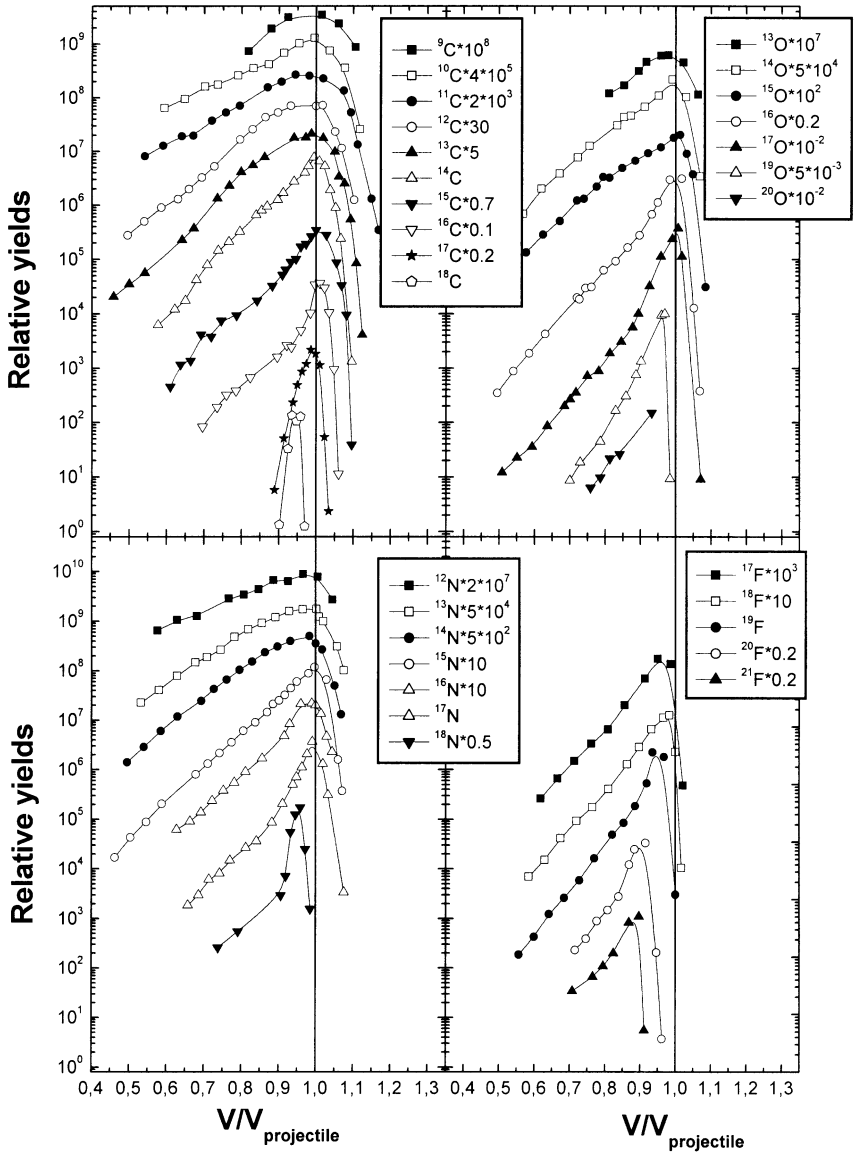

Fig.5. The forward-angle inclusive velocity distributions (relative yields) of the isotopes C, N, O and F. The isotope velocity V is referred to that of the beam $V_{projectile}$. The numbers near isotopes (in frame) show the multiplied factors of the experimental yields (for visual convenience).

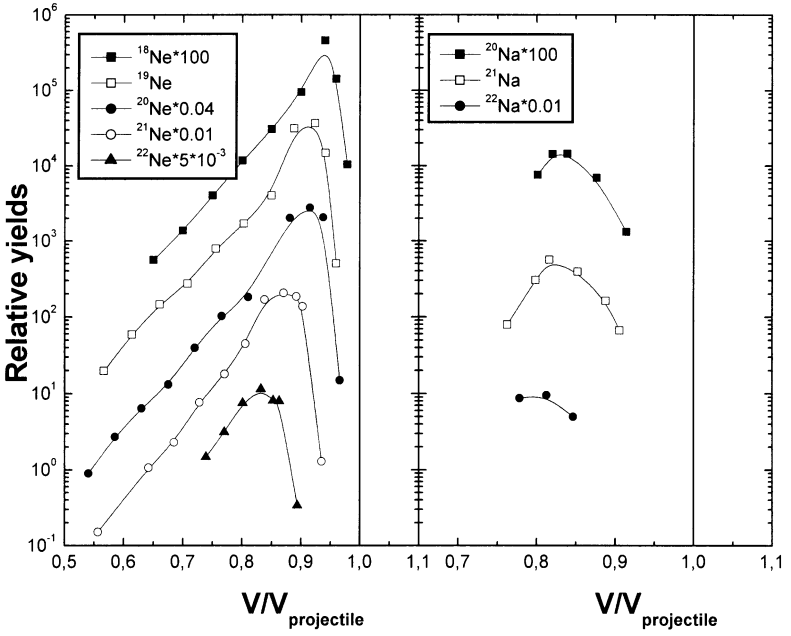

Fig.6. The forward-angle inclusive velocity distributions (relative yields) of the isotopes Ne and Na. The isotope velocity V is referred to that of the beam $V_{projectile}$. The numbers near isotopes (in frame) show the multiplied factors of the experimental yields (for visual convenience).

the projectile $V_{projectile}$. The existence of different reaction mechanisms can be observed by the evolution of the shape of the isotopic velocity distributions while the increase of the number of the transferred nucleons.

Figs.3a and 3b demonstrate the velocity distributions for the two extreme cases obtained: in small nucleon transfer (Fig.3a) and in multinucleon transfer (Fig.3b) corresponding to the weakly-bound nuclei produced near the neutron drip-line. Nuclear reaction products of the mass close to the mass of the projectile (^{16,17,19}O, ^{17,18}N, ^{16}C, small nucleon transfer) are characterized by a narrow bell-like shape with a maximum close to the projectile velocity. The visual shift of the velocity maxima of the ^{18}N and ^{19}O isotopes produced in the neutron pick-up reaction is of kinematic origin (see below). Gaussian-like velocity distributions of such a shape are observed in small nucleon transfer reactions at low energy (quasi-elastic transfer). The shape of the velocity distributions in the range of the less velocity (Fig.3a) shows a bend at the level of more than 100 below maximum yield, and then a slower exponential fall is observed. The contribution of this slower fall component (inelastic portion of the spectrum) to the total yield of the isotope increases noticeably while the number of transferred nucleons increases.

The group of weakly-bound isotopes (Fig.3b) is characterized by a gaussian-like single-component shape which is symmetrically concentrated around the projectile velocity. The widths of the velocity distributions for those isotopes tend to increase as the number of transferred nucleons increases. The shape of the velocity distributions of those weakly-bound nuclei is close to the shape of the quasi-elastic component in the yields of isotopes obtained in the small nucleon transfer (Fig.3a). As seen from Fig.3b, there is no inelastic compo-

nent in the yields of these nuclei in spite of the massive nucleon transfer they are produced in. Evidently this is due to the decay of weakly-bound nuclei produced in inelastic processes with the noticeable excitation energy.

More complicated velocity distributions are observed for the intermediate case of massive nucleon transfers (Fig.4, 5 and 6). The isotopes around the stability line and proton rich isotopes produced in more massive stripping nucleons are characterized by asymmetric shapes. The maximum yields are concentrated near the projectile velocity (except the alpha particle distribution) and tend to broadening of distributions while the number of the transferred nucleons increases. The contribution of inelastic components (low-velocity sides) increases appreciably as the number of the transferred nucleons increases (tails are flattened). This growing contribution of the exponential tails from the low-velocity side to the total yields of these isotopes demonstrates the increasing role of the dissipative processes as well as of secondary deexcitation processes.

The velocity distributions of isotopes produced in the nucleon pick-up reactions or nucleon exchange reactions (isotopes ^{19,20,21}F, $^{18-22}$Ne, ^{17,18}C, ^{18}N, ^{19}O) are similar by the shapes to those of the intermediate group except the position of maximum. The maxima of these distributions are concentrated on the velocities less than the projectile velocity tending to the systematic shift as the number of the pick-up protons and neutrons increases. These phenomena are of kinematic origin due to the slowing down velocity of isotopes with pick-up of nucleons. The growing contribution of the low energy tails, as the number of the pick-up nucleons increases, demonstrates the increasing role of dissipative processes in the nuclei production.

3.2 Isotopic distribution of the products

To produce the isotopic distributions, the velocity-distributions were integrated in the measured region of velocities (Fig.7a) . In the oxygen isotopic distribution the yield of ^{18}O isotope was excluded because it was impossible to separate the reaction yield of ^{18}O from ^{18}O projectile.

For each element the isotopic distributions are similar to the bell-like shapes excluding the He and Li distributions. The most probable yields correspond to masses around stability line isotopes. The sharp exponential decrease in the yields of heavy isotopes for each element is observed. The light isotope side of distributions increases as the number of stripping protons increases. The isotopic distributions of Li and He elements produced with a maximum number of stripping protons and neutrons are degenerated in the exponential shape. Accumulation of the lightest isotopes (proton rich) for each element, especially for the lightest elements, is affected by the contributions of evaporative lightest particles. This correlates with the behaviour of growing contributions of the low-energy part of velocity distributions of these isotopes.

3.3 Element distributions of the products

The element distributions (Z-distributions) were obtained by integration of isotopic distributions (Fig.7b) . The yield of the Z=8 element (projectile) is underestimated due to the unknown yield of the ^{18}O reaction production.

For the products with Z greater than Z of the projectile, the production yields decrease with increasing Z. A weak odd-even effect (enhancement of carbon)is also visible in the Z-distribution. The striking feature of the pro-

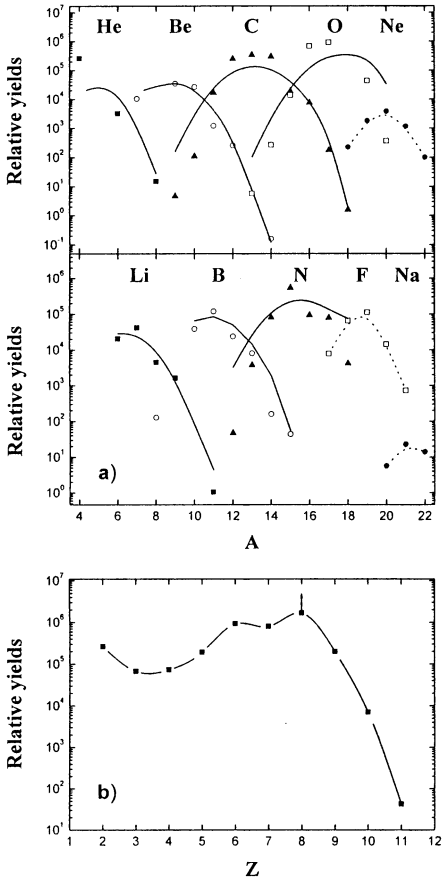

Fig.7. a) The isotopic distributions obtained by integration of velocity distributions versus the detected mass A. The yield of the ^{18}O isotope is excluded due to the impossibility to separate the reaction production of ^{18}O from ^{18}O projectile. The solid lines present the LISE code fit (see the text). The dotted lines for the F, Ne and Na isotopic distributions induced in the proton pick-up reactions are drawn for visual convenience through the experimental yields. **b)** The element distributions (Z - distributions) versus the atomic number. The yield of the Z=8 element (projectile) is underestimated due to unknown yields of the ^{18}O reaction production.

duced Z-distribution is that within a factor of five all the elements from Z=2 till Z=7 are equally produced. The sharp increasing of yield of the lightest elements with Z$\leq$2 is observed.

4 Discussion of the results

The evolution of the velocity and isotopic distributions produced in forward-angle measurements versus the number of transfer nucleons have shown the existence of different reaction mechanisms.

In the Fermi energy domain (35·A MeV) the velocity distribution of the isotopes close to the projectile demonstrates a dominant role of direct peripheral reactions like binary processes of the stripping and pick-up of several nucleons in the low energy region [2, 15]. The main contribution of these reactions is observed in the yields of all the isotopes including the isotopes induced in the reactions with a massive transfer of nucleons. In the production of the weakly-bound nuclei of ^{8}He, ^{11}Li, ^{12}Be, ^{14}Be and ^{15}B the peripheral binary reactions also play a dominant role. These drip-line nuclei are produced in nuclear reactions with the maximum number of the transferred protons.

The analysis of the velocity distributions of the detected fragments within the framework of the simple fragmentation model has shown that there is disagreement with the experimental data obtained in forward-angle measurements.

A naive picture of geometric fragmentation predicts the regular decreasing of velocity of isotopes with the increasing of the number of removed

nucleons [1, 6]:

$$V/V_p = \left[(35 \cdot A - (A_p - A) \cdot 8)/35 \cdot A_p\right]^{1/2} \cdot (A_p/A)^{1/2}, \qquad (3)$$

where A_p, V_p and A, V mean the mass numbers and velocities of the projectile ^{18}O with 35·A MeV and the isotope, accordingly; 8 MeV is the average energy of a single removed nucleon. As seen from Fig.3b), the experiment has not confirmed the systematic drift of the maximum of the velocity distributions to lower velocities with the increasing number of the removed protons predicted by the fragmentation model.

For example, the relative yields of isotopes of Be calculated by using the LISE code based on the fragmentation hypothesis[16] are presented on the Fig.8. There is no agreement between the prediction and the experiment on the shape and, especially, on the position of the maximum. The discrepancy between the predicted shape of the magnetic rigidity distributions and the experimental data increases for heavier isotopes. For the drip-line isotope ^{14}Be the widest distribution is predicted and the centroid is considerably shifted to smaller magnetic rigidity. The observed discrepancy on the shape and position of maximum for the drip-line nuclei should be taken into account in the experiments being planned, especially when a small-momentum acceptance fragment separator is used. Fig.7a) presents the degree of agreement of the calculated fit by LISE code with the experimental data of isotopic yields.

In addition, the production of isotopes with $Z > Z_{projectile}$(F, Ne and Na) is not conceptually assumed on the projectile fragmentation hypothesis. On the Fig.6 the experimental points for these isotopes are connected in the dotted curve to guide the eye.

It is known [17] that in the low energy region the yields of isotopes pro-

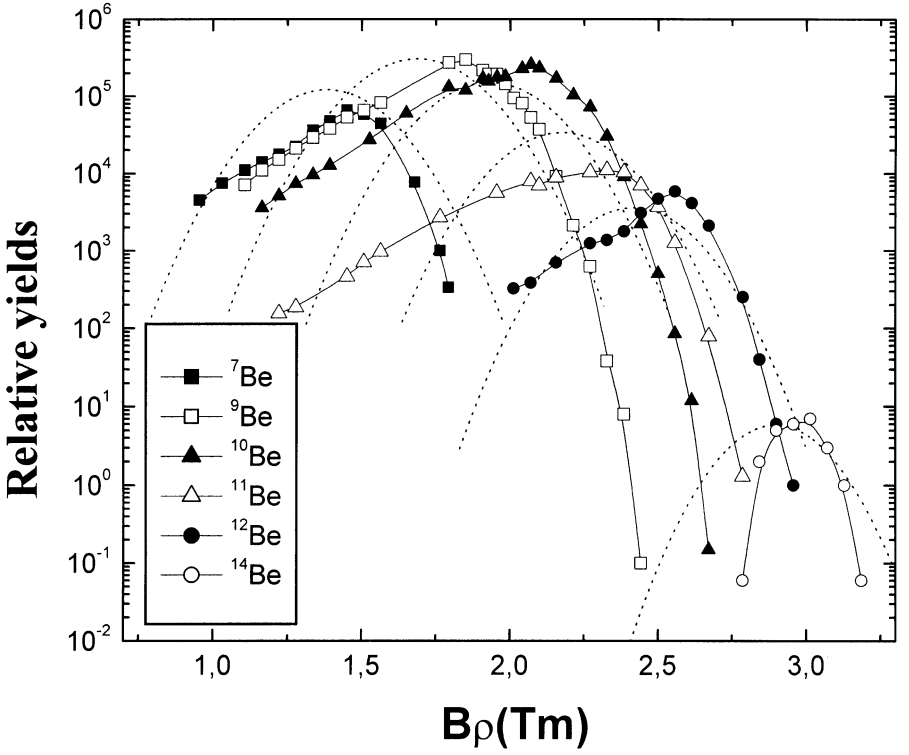

Fig.8. The yield distributions of the Be isotopes versus the magnetic rigidity Bρ (in Tm). The solid lines are drawn for visual convenience through the experimental points. The dotted lines present the LISE code fit (see the text).

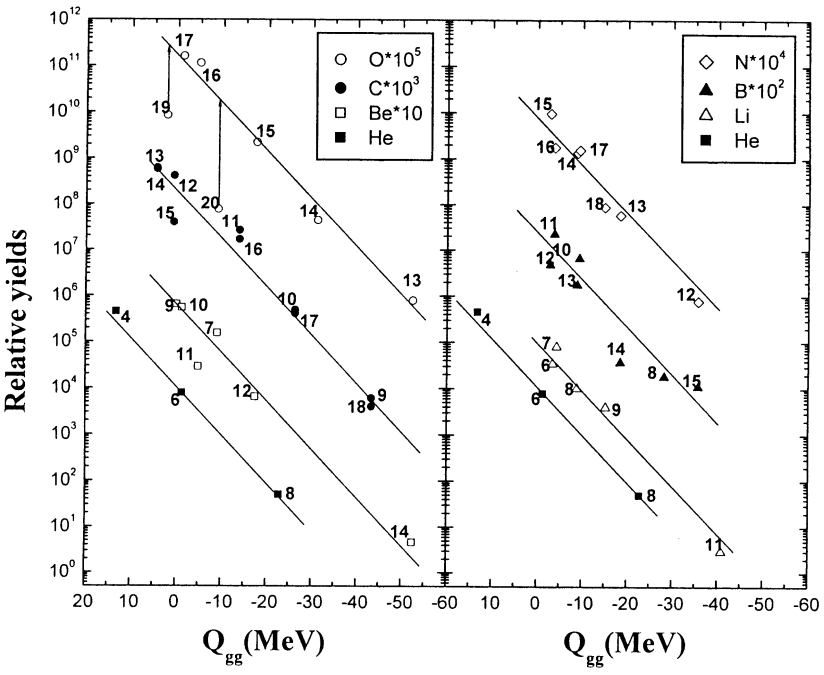

Fig.9. The isotopic yields of elements with $2 \leq Z \leq 10$ versus the Q_{gg} - values (the Q_{gg}-systematics). The value Q_{gg} is $(M_p + M_t)$ - $(M_{det} + M_{undet})$, where M_p, M_t, M_{det} and M_{undet} are the ground state masses of the projectile, target, detected isotope and undetected isotope (the partner of detected isotope in the exit channel of the reaction), accordingly. Arrows for the isotopes O, F and Ne show the decrease in the yields of the isotopes as a possible consequence of the influence of the deexcitation effects. The numbers near isotopes (in frame) show the multiplied factors of the experimental yields (for visual convenience).

duced in stripping reactions can be approximated with a simple exponential function of Q_{gg}:

$$y = C \cdot \exp(Q_{gg}/T), \tag{4}$$

where T is the parameter in MeV determining the slope of the exponent and C is the constant.

The Q_{gg} - systematics characterizing the binary type of isotopic production is given in Fig.9. In the calculation of Q_{gg} it is assumed that there are two particles (projectile and target) in the entrance channel and two particles (detected fragment and undetected residue of the composite system) in the exit channel. Q_{gg} value is determined by the difference of the ground state (g. s.) masses of the partners before and after the collision.

It is seen from Fig.9 that the simple exponential approximation realized by the Q_{gg} - systematics describes the total yield of the isotopes produced in stripping nucleon reactions with large negative Q_{gg} values. The uniqueness of the Q_{gg} - systematics consists in the satisfactory description of the isotopic yields of all the elements by the same simple exponent in the range more than five orders. Q_{gg} - systematics is a powerful tool to predict correctly the expected yields of the unknown drip-line nuclei in the experimental search. As seen from Fig.9, the decrease of the yields of the detected isotopes in comparison with the averaged Q_{gg} - exponent is observed in the range of the small negative or positive Q_{gg} -values. The largest discrepancy is observed for heavy isotopes of ^{19}O and ^{20}O produced in the neutron pick-up reactions. It is known that each nucleon pick-up deposits energy excitation in nucleus-acceptor. That is why the observed decrease of yields for pick-up neutron nuclei can be due to a consequence of the deexcitation effects. The reduction

of the detected yields of separate isotopes of ^{11}Be, ^{14}B and ^{15}C can be caused by their structure favouring to disintegration.

The experiment was also carried out to estimate the production rates of halo-like nuclei of ^{11}Li ($6{\cdot}10^3$ pps), ^{12}Be ($3{\cdot}10^5$ pps) and ^{14}Be ($5{\cdot}10^2$ pps) induced by the 630 MeV ^{18}O beam on the 200-mg/cm^2 ^{9}Be target. The primary beam current on the target reached 10 μAe. The achromatic spectrometer COMBAS was used with the total momentum ($\pm$10%) acceptance and total solid angle (6.4 mstr).

5 Conclusion

The production of isotopes with the mass numbers $4 \leq A \leq 22$ and atomic numbers $2 \leq Z \leq 11$ induced in the inverse kinematic reaction ^{18}O + ^{9}Be in the Fermi energy domain (35·A MeV) has been studied in forward-angle measurements by using the kinematic double achromatic separator COMBAS.

No evidence was found for any dramatic change of the reaction mechanism for peripheral reactions in comparison with the same in the low energy range. In the beam direct selection of isotopes induced in the interaction of light projectile and light target, the dominant role of stripping, pick-up and exchange nuclear reactions is observed. Considerable contributions from dissipative processes are found for isotopes around the stability line. The united exponential approximation by using the Q_{gg} - systematics of isotopic distributions for all detected elements, has confirmed the binary type of the reaction production of neutron-rich isotopes. The simple exponential ap-

proximation realized by the Q_{gg} - systematics is a powerful tool to predict correctly the expected yields of unknown drip-line nuclei.

It is shown that LISE code underestimates the yields and incorrectly predicts the characteristics of velocity distributions of drip-line isotopes (width and maximum position) and this fact should be taken into account for the experiments on the synthesis of unknown drip-line isotopes by using a fragment-separator with small momentum acceptances. The observed intensive production of isotopes with the atomic number larger than the projectile ($Z > 8$) contradicts to the projectile fragmentation hypothesis.

The production rates of exotic nuclei of ^{9}Li, ^{11}Li, ^{11}Be, ^{12}Be and ^{14}Be have been determined, that could be used as secondary radioactive beams of halo-like nuclei.

It would be very important to continue the study of the evolution of reaction mechanisms as a function of the projectile energy as well as of the target neutron excess $(N/Z)_t$.

6 Acknowledgments

This work was supported in part by grant INTAS-93-496 and by grant RFBR-96-02-17214. The authors are indebted to Prof. Yu.Ts. Oganessian for fruitful discussions and support of this work. We also thank A.V. Solodovnikov for the assistance during the run and V.E. Zhuchko and V.S. Salamatin for the data acquisition and processing programmes.

Appendix. Forward-angle spectrometry of charged reaction products.

For kinematic reasons (especially for inverse kinematic reactions), the angular distributions of the reaction products induced by intermediate energy projectiles are strongly focused in the beam direction. Moreover, in zero angle studies the elastic scattering on entrance slits, elastic scattering on light target contaminants and especially ghost beam (halo) are the main experimental problems which lead to a lot of extensive "background" testing measurements. The requirements on the quality of the ion-optical parameters of the beam (minimum size and minimum angular divergence) also increase considerably when performing measurements as close to the beam [11, 18] as possible.

In heavy ion collisions, the narrow angular structure is occupied by various reaction mechanisms due to the existence of a band of angular momenta inducing different reaction mechanism components. The forward peaked angular distributions are resulting from quasi-elastic reactions, direct processes of transfer nucleons, peripheral dissipative processes, projectile-like and target-like fragments and complete fusion reactions. Therefore highly accurate angular measurements could be a probe of the reaction mechanisms.

The most important parameters governing the forward-angle physics are presented below.

1) Following the one-quarter point technique [19] the grazing angle θ_{gr} is presented by the ratio of the experimental elastic cross section to Rutherford cross section $\sigma_{el}(\theta_{cm})/\sigma_{Ruth}(\theta_{cm}) = 1/4$ from which is obtained the simple

relation

$$\sin\left(\frac{\theta_{cm}^{gr}}{2}\right) = \eta/(kR - \eta). \tag{5}$$

Here $\eta = (Z_p \cdot Z_t)/137 \cdot \beta$ is the Coulomb parameter showing the a scaling of the Coulomb effects and β is the ratio of the relative incident velocity to that of light and k is the wave number.

Within the small-angle approximation in the laboratory frame

$$\theta_{Lab}^{gr} \approx \frac{1.44 \cdot Z_p \cdot Z_t}{R \cdot E_p}(rad), \tag{6}$$

where the subscripts p and t refer to the projectile and the target, respectively, and $R = r_0 \cdot \left(A_p^{1/3} + A_t^{1/3}\right)$ the radius of interaction (fm) and E_p is the total projectile energy (MeV).

2) The scaling of the nuclear effects can be approximately modeled by the value of the fragmentation angle $\theta_{frag}(\Delta A) = \sigma_{p\perp}/P_{//}$ [1,3], which is characterized by the mean square total momentum of the residue A_p - ΔA when ΔA random nucleons are removed from the projectile A_p. Here $\sigma_{p\perp}$ is the variance of the isotope traverse momentum and $P_{//}$ is the longitudinal momentum component of residue, accordingly.

Within the small-velocity changes [11] (high energy fragmentation limit) the $\theta_{frag}(\Delta A)$ can be approximated by following simple relation

$$\theta_{frag}(\Delta A) \approx \frac{\sigma_0}{\sqrt{2m_0}}\sqrt{\frac{\Delta A \cdot A_p}{(A_p - \Delta A) \cdot E_p (A_p - 1)}}(rad), \tag{7}$$

where m_0 is the nucleon mass in MeV/c^2 and $\sigma_0 = 80$ MeV/c is related to the Fermi momentum P_F by following expression $\sigma_0^2 = 1/5 \cdot P_F^2$ [1].

3) The angular structure can also broaden by evaporation of an ejectile of mass A_{ev} in a random direction with the energy E_{ev} before the detection of the final mass products A_{res}. The mean evaporation angle θ_{ev} can be evaluated [11] using the simple relation

$$\theta_{ev}\left(A_{ev}, E_{ev}, A_{res}\right) \approx \frac{\pi}{4} \cdot \sqrt{\frac{A_{ev} \cdot E_{ev}}{A_{res}^2 \cdot E_p/A_p}}(rad). \tag{8}$$

4) The minimum width to be achieved in angle measurements $\Delta\theta_{min}$ can be estimated using the uncertainty principle for the conjugated variables of the angle $\Delta\theta$ and of the angular momentum ΔL from the relation $\Delta\theta \cdot \Delta L \approx 1$ (wave-packet uncertainty), where ΔL is the band of the angular momentum related to the grazing angular momentum of the collision. Therefore the smallest width which can be found in the angular structure can be expressed as follows:

$$\Delta\theta_{\min}\left(A_F\right) \approx \frac{1}{L_{gr}} \approx \frac{4.55}{r_0 \cdot \left(A_p^{1/3} + A_t^{1/3}\right) \cdot \sqrt{E_p/A_p} \cdot A_F}(rad). \tag{9}$$

5) The main atomic broadening effects are associated with the slowing down processes in target as called the angular straggling and the energy straggling. The angular straggling for heavy ions up to 100 MeV/A can be expressed with a good accuracy using the scaling law

$$\langle\delta\theta\rangle = 1.0 \cdot \tau^{0.55}. \tag{10}$$

Here $\langle\delta\theta\rangle$ and τ are reduced variables linking the angular straggling $\delta\theta$ (half width at half maximum of the angular distribution) and to the target thickness t through the relations [20]:

$$\langle\delta\theta\rangle = 16.26 \cdot \frac{E}{Z_p \cdot Z_t \cdot \left(Z_p^{2/3} + Z_t^{2/3}\right)^{1/2}} \cdot \delta\theta \tag{11}$$

and

$$\tau = \frac{41.5 \cdot 10^3 \cdot t}{A_t \cdot \left(Z_p^{2/3} + Z_t^{2/3}\right)}, \tag{12}$$

in which t is expressed in mg/cm^2 and E in MeV and $\delta\theta$ in mrad.

The energy loss straggling for fully stripped projectile is usually expressed by the Bohr variance [21]

$$\delta E^2 = 1.57 \cdot 10^{-4} \cdot \frac{Z_p^2 \cdot Z_t \cdot t \cdot (1 - \beta^2/2)}{A_t \cdot (1 - \beta^2)}. \tag{13}$$

The simplified version with a good accuracy can be presented by the following expression

$$\delta E \approx K \cdot Z_p \cdot \sqrt{\frac{Z_t}{A_t} \cdot t(inMeV)}, \tag{14}$$

where target thickness t is g/cm^2, and $K = 2.0$.

The most important parameters governing the forward-angle physics for the studied reaction ^{18}O (35 $\cdot$ A MeV) + ^{9}Be are shown below. In Table the parameters for the more asymmetry reaction ^{18}O (35 $\cdot$ A MeV) + ^{181}Ta are presented also (for comparison).

θ (mrad) Lab. System	^{18}O ($E_p = 35 \cdot$ A MeV)	
	$^{9}_{4}Be$	$^{181}_{73}Ta$
θ_{gr}	11.0	115.2
θ_{frag} (4)	35.5	35.5
θ_{frag} (9)	66.5	66.5
$\theta_{e\nu,1}$ (2, 3, 16)	20.3	20.3
$\theta_{e\nu,2}$ (4, 5, 9)	66.0	66.0
$\Delta\theta_{min}$ (18)	6.5	3.7
$\Delta\theta_{min}$ (9)	13.0	7.4
Stragglings	$^{9}_{4}Be$ (14.0 mg/cm^2)	$^{181}_{73}Ta$ (14.0 mg/cm^2)
δE (MeV)	1.3	1.2
$\delta\theta$ (mrad)	3.2	7.42

where θ_{gr}, θ_{frag}, $\theta_{e\nu}$, $\Delta\theta_{min}$, δE and $\delta\theta$ are the grazing angle, fragmentation angle, evaporation angle, minimum angular structure, energy straggling and angular straggling, accordingly.

References

[1] B.Borderie, M.F.Rivet and L.Tassan-Got, Ann. of Phys. 15(1990)287

[2] M.Lefort and Ch.Ngo, Ann. of Phys. 3(1978)5

[3] A.S.Goldhaber and H.H.Heckman, An. Rev. Nucl. Part. Sci. 28(1978)161

[4] D.Guillemaud-Mueller, Yu.E.Penionzhkevich, R.Anne, A.G.Artukh, D.Bazin et al., Z. Phys., A332(1989)189

[5] H.Sakurai, N.Aoi, D.Beaumel, N.Fucuda, M.Hirai et al., Proc. of 4th Int. Conf. on Rad. Nucl. Beams, Omiya, 1996, ed. S.Kubono, T.Kobayashi and I.Tanihata (Elsevier, Amsterdam, 1997), p. 311.

[6] V.Borrel, D.Guerreau, J.Galin, B.Gatty, D.Jacquet and X.Tarrago, Z. Phys., A314(1983)191.

[7] Y.Blumenfeld, PH.Chomaz, N.Frascaria, J.P.Garron, J.C.Jacmart et al., Nucl. Phys., A455(1986)357.

[8] V.Borrel, B.Gatty, D.Guerreau, J.Galin and D.Jacquet, Z. Phys., A324(1986)205.

[9] M.C.Mermaz, V.Borrel, D.Guerreau, J.Galin, B.Gatty and D.Jacquet, Z. Phys., A324(1986)217.

[10] D.Bazin, D.Guerreau, R.Anne, D.Guillemaud-Mueller, A.C.Mueller and M.G.Saint-Laurent, GANIL report P89-22(1989).

[11] Ch.O.Bacri, P.Roussel, V.Borrel, F.Clapier, R.Anne et al., Nucl. Phys., A555(1993)477.

[12] A.G.Artukh, G.F.Gridnev, M.Grushezki, F.Koscielniak, A.G.Semchenkov et al., Nucl. Instr. and Meth., A426(1999)605.

[13] A.G.Artukh, G.F.Gridnev, V.L.Mikheev and V.V.Volkov, Nucl. Phys., A137(1969)348.

[14] A.G.Artukh, V.V.Avdeichikov, J.Ero, G.F.Gridnev, V.L.Mikheev et al., Nucl. Instr. and Meth., V83(1970)72.

[15] A.G.Artukh, G.F.Gridnev, V.L.Mikheev, V.V.Volkov and J.Wilczynski, Nucl. Phys., A215(1973)91.

[16] D.Bazin and O.Sorlin, private communications; WEB site - http://www.nscl.msu.edu/~bazin/LISE.html and modified WEB site - http://dnr080.jinr.ru/LISE.html.

[17] A.G.Artukh, V.V.Avdeichikov, J.Ero, G.F.Gridnev, V.L.Mikheev, V.V.Volkov and J.Wilczynski, Nucl. Phys., A160(1971)511.

[18] Ch.O.Bacri and P.Roussel, Nucl. Instr. and Meth., A300(1991)89.

[19] W.E.Frahn, Ann. of Phys., 72(1972)524.

[20] R.Anne, J.Herault, R.Bimbot, H.Gauvin, G.Bastin and F.Hubert, Nucl. Instr. and Meth., B34(1988)295.

[21] J.Herault, R.Bimbot, H.Gauvin, B.Kubica, R.Anne, G.Bastin and F.Hubert, Nucl. Instr. and Meth., B61(1991)156.

Received by Publishing Department
on December 20, 2000.

Артюх А.Г. и др. E7-2000-305

Выходы изотопов под углом 0° к пучку с $2 \le Z \le 11$ в реакции ^{18}O (35 · A МэВ) с ядрами ^{9}Be

Проведены систематические исследования образования широкого спектра изотопов под углом 0° к пучку с $2 \le Z \le 11$ в ядерной реакции ^{18}O с ядром ^{9}Be при энергии столкновения 35 · A МэВ (энергия Ферми). Выходы продуктов ядерных реакций были измерены дважды ахроматическим кинематическим сепаратором КОМБАС (ЛЯР ОИЯИ, Дубна) в спектрометрическом варианте. Исследования скоростных, изотопных и элементных распределений продуктов выявили доминирующую роль механизмов ядерных реакций, характерных для реакций с тяжелыми ионами при низких энергиях. Определены интенсивности вторичных пучков галоподобных ядер ^{11}Li, ^{12}Be и ^{14}Be.

Работа выполнена в Лаборатории ядерных реакций им. Г.Н.Флерова ОИЯИ.

Препринт Объединенного института ядерных исследований. Дубна, 2000

Artukh A.G. et al. E7-2000-305

Forward Angle Yields of Isotopes with $2 \le Z \le 11$ in the Reaction of ^{18}O (35 · A MeV) with ^{9}Be

Systematic investigations of forward-angle inclusive yields of isotopes with atomic numbers $2 \le Z \le 11$ produced in nucleus-nucleus collisions of the ^{18}O projectile and the ^{9}Be target in the Fermi energy region (35 · A MeV) have been carried out. The measurements have been performed by using the double achromatic kinematic separator COMBAS in the spectrometry mode at the FLNR, JINR (Dubna). The velocity, isotopic and element distributions are presented. There is no unique reaction mechanism to explain the total set of the results obtained from the experiment. A dominant role of low energy reaction mechanisms is observed. The intensity of secondary beams of halo-like nuclei ^{11}Li, ^{12}Be, and ^{14}Be is determined.

The investigation has been performed at the Flerov Laboratory of Nuclear Reactions, JINR.

Preprint of the Joint Institute for Nuclear Research. Dubna, 2000

Макет Т.Е.Попеко

Подписано в печать 12.02.2001
Формат 60 × 90/16. Офсетная печать. Уч.-изд. листов 2,79
Тираж 315. Заказ 52495. Цена 3 р. 35 к.

Издательский отдел Объединенного института ядерных исследований
Дубна Московской области